

Structural Variability and the Nature of Intermolecular Interactions in Watson–Crick B-DNA Base Pairs

Ż. Czyżnikowska,^{*,†,‡} R. W. Góra,[†] R. Zaleśny,[†] P. Lipkowski,[†] K. N. Jarzembska,[§]
P. M. Dominiak,[§] and J. Leszczynski[‡]

Theoretical Chemistry Group, Institute of Physical and Theoretical Chemistry, Wrocław University of Technology, Wyb. Wyspińskiego 27, 50-370 Wrocław, Poland; Interdisciplinary Center for Nanotoxicity, Department of Chemistry, Jackson State University, 1400 J. R. Lynch St., Jackson, Mississippi 39217; and Department of Chemistry, Warsaw University, Pasteura 1, 02-093 Warsaw, Poland

Received: February 9, 2010; Revised Manuscript Received: June 14, 2010

A set of nearly 100 crystallographic structures was analyzed using ab initio methods in order to verify the effect of the conformational variability of Watson–Crick guanine–cytosine and adenine–thymine base pairs on the intermolecular interaction energy and its components. Furthermore, for the representative structures, a potential energy scan of the structural parameters describing mutual orientation of the base pairs was carried out. The results were obtained using the hybrid variational–perturbational interaction energy decomposition scheme. The electron correlation effects were estimated by means of the second-order Møller–Plesset perturbation theory and coupled clusters with singles and doubles method adopting AUG-cc-pVDZ basis set. Moreover, the characteristics of hydrogen bonds in complexes, mimicking those appearing in B-DNA, were evaluated using topological analysis of the electron density. Although the first-order electrostatic energy is usually the largest stabilizing component, it is canceled out by the associated exchange repulsion in majority of the studied crystallographic structures. Therefore, the analyzed complexes of the nucleic acid bases appeared to be stabilized mainly by the delocalization component of the intermolecular interaction energy which, in terms of symmetry adapted perturbation theory, encompasses the second- and higher-order induction and exchange-induction terms. Furthermore, it was found that the dispersion contribution, albeit much smaller in terms of magnitude, is also a vital stabilizing factor. It was also revealed that the intermolecular interaction energy and its components are strongly influenced by four (out of six) structural parameters describing mutual orientation of bases in Watson–Crick pairs, namely *shear*, *stagger*, *stretch*, and *opening*. Finally, as a part of a model study, much of the effort was devoted to an extensive testing of the UBDB databank. It was shown that the databank quite successfully reproduces the electrostatic energy determined with the aid of ab initio methods.

Introduction

The stability and conformation of biomacromolecules are influenced by numerous factors. For this reason and due to the large size of such molecules, molecular modeling of biomacromolecules still remains a challenging task for biophysicists and computational chemists. Various components of nucleic acid, nucleic acid–protein, and nucleic acid–drug complexes are involved in two qualitatively different interaction types: hydrogen bonding and stacking. These interactions are responsible for a vital biological functions. For instance, the formation of pairs of complementary sequences of DNA and RNA is due to the unique molecular recognition of nucleic acid bases (NABs) via hydrogen bonds. These interactions are also significant for stabilization of higher-order structures of nucleic acids.^{1–4}

Many computational studies characterizing the hydrogen-bonding and stacking interactions between native and modified nucleic acid bases have been performed and the number of computational studies grows rapidly every year.⁵ Various aspects of intermolecular interactions in nucleic acids such as base pairing, interactions with metal cations, base triples and

quadruples creation, and water-connected pairs formation have been the main subject of interest of such studies. Besides, pairs of modified and protonated bases have been studied with the state of the art ab initio methods.^{6–13} However, not much attention has been paid to the nature of intermolecular interactions in biologically important complexes. In fact, the majority of computational studies concerned with the physical origins of stabilization was performed for stacked configurations of native and oxidized complexes of nucleic acid bases.^{14–21} The nature of interactions in hydrogen-bonded Watson–Crick base pairs seems not to be of a great interest.^{21–27} The most relevant studies to the analysis of nature of interactions in the hydrogen-bonded NAB complexes are briefly discussed below.

The studies of Toczyłowski and Cybulski^{25,26} are of particular importance for the analysis of the nature of intermolecular interactions in NAB complexes. In order to elucidate the interplay of various interaction energy components, the authors used interaction energy partitioning scheme based on intermolecular Møller–Plesset perturbation theory.^{28,29} They examined over 30 hydrogen-bonded nucleic acid base pairs; however, the parameters describing the intermolecular geometry of these complexes were not exactly the same as those corresponding to the structures found in native DNA. Nevertheless, their studies provided valuable insights regarding the physical origins of

* Corresponding author. E-mail: zaneta.czynikowska@gmail.com.

† Wrocław University of Technology.

‡ Jackson State University.

§ Warsaw University.

stabilization of H-bonded NAB complexes. They analyzed Watson–Crick, reversed Watson–Crick, Hoogsteen, and reversed Hoogsten pairs. On the basis of the potential energy scan in the vicinity of the minimum, they concluded that the small changes of intermolecular distance have only slight impact on the stabilization energy. On the other hand, even small changes of the angular parameters influence significantly the intermolecular interaction energy. Especially, the Heitler–London exchange energy was identified as the most anisotropic component. A key point raised by Toczyłowski and Cybulski is that the first-order electrostatic energy, which is the largest component of the interaction energy in terms of its magnitude, is significantly quenched by the Heitler–London exchange component. Likewise, the dispersion energy was found to be canceled out to a large extent by correlation correction to the exchange energy. More recently, similar trends were observed by Hesselmann and co-workers who used DFT-SAPT approach in the density fitting approximation.²³ They reported, that the Watson–Crick guanine–cytosine (G-C) and adenine–thymine (A-T) complexes that were analyzed by them are mainly stabilized by first-order electrostatics. However, the authors also reported that this component is compensated by the first-order exchange repulsion energy. As it turns out, in a majority of crystallographic structures analyzed in the present study the first-order electrostatic interaction energy was in fact completely canceled out by the associated exchange repulsion.

The most of systematic state of the art ab initio calculations of nucleic acid base complexes were carried out by Hobza and collaborators. They focused mainly on the calculations of accurate intermolecular interaction energies at the MP2, MP3, and CCSD(T) levels of theory.^{30–35} The gathered data, although of indisputable significance for analyzing nucleic acid base complexes, does not provide much insight into the physical origins of interactions in the studied complexes. Recently, this group performed an analysis of the nature of intermolecular interactions for a set of nine Watson–Crick A-T base pairs.²⁴ The interaction energy components were estimated using DFT-SAPT approach. The authors reported that the first-order electrostatic energy plays a key role in stabilization of the investigated complexes. However, they concluded that the other interaction energy components are also important. For instance, they found out that the sum of the second-order components (i.e., dispersion and induction energies) in the investigated complexes amounts to about 56% of the contribution due to the first-order electrostatic interaction. Generally, their results²⁴ are consistent with those reported by Toczyłowski and Cybulski.²⁵

Many different qualitative models have been proposed in the literature to describe strong hydrogen bonds like the ones formed between NABs pairs. One particularly interesting is the electrostatic-covalent HB model proposed by Gilli and co-workers.³⁶ They suggested the dual nature of hydrogen bonds: electrostatic and covalent, and provided evidence of the significance of covalent character of hydrogen bonds. They postulated also that a strong character of hydrogen bonds in nucleic acid base pairs is connected not only with the electrostatic interactions but also with the formation of the so-called resonance-assisted hydrogen bonds (RAHB).^{36–38} Surprisingly, there are not many studies devoted strictly to Bader's quantum theory of "atoms in molecules" (QTAIM) analysis of hydrogen bonds formed between NABs pairs. Only recently, the strength of hydrogen bonds in 15 nucleic acid base pairs have been investigated by Mohajeri et al.³⁹ On the basis of the correlations observed between various structural, energetic, and QTAIM descriptors,

the authors suggested that almost all analyzed Watson–Crick base pairs are stabilized by medium-strength hydrogen bonds.

The present study is aimed at a more systematic analysis of the nature of intermolecular interactions in NAB complexes in conformations appearing in B-DNA crystals. In order to avoid bias due to a limited set of structures, we selected almost 100 crystallographic structures of guanine–cytosine and adenine–thymine Watson–Crick base pairs. Furthermore, for the most representative structures, we performed a potential energy scan of the structural parameters describing mutual orientation in Watson–Crick pairs, namely *shear*, *stagger*, *stretch*, *opening*, *buckle*, and *propeller*. The rationale for selecting two different sets of molecular geometries arises from the fact that the former approach allows to study the interactions in experimentally observed conformations while the latter might help to analyze the anisotropy of intermolecular interactions in a systematic manner. Our study should provide a better understanding of the physical origins of the stabilization of NAB complexes and the anisotropy of intermolecular interaction energy (hereafter abbreviated as IIE) and its components. Moreover, we wish to investigate the effect of the structural variability of Watson–Crick base pairs on the strength of the hydrogen bonds formed, by employing the QTAIM theory. Among various approaches used for estimation of the hydrogen bond strength, Bader's quantum theory of atoms in molecules is one of the most common.⁴⁰ Since the NAB complexes that are studied in this paper are connected via hydrogen bonds, we believe it is appropriate to supplement our studies with the results of QTAIM analysis, particularly since it is well established that, for hydrogen-bonded complexes, the QTAIM protocol provides an unambiguous and very efficient view of intermolecular phenomenon.^{40–42}

Despite the recent progress in computational chemistry^{43–45} and biophysics, it is still very difficult to accomplish reliable predictions of the nature of intermolecular interactions in NAB complexes with the inclusion of electron correlation as well as solvent and entropic effects. The complexity and size of biomolecular systems are the factors which hamper the application of high-level ab initio quantum chemistry methods and prompt the development of computationally less demanding techniques. Very accurate values of intermolecular interaction energy, and its components, can be obtained for relatively small complexes only.^{46–48} Therefore, evaluating the nature of interactions in large polynucleotide fragments requires more approximate treatments. A good example of such an approach is the combination of the University at Buffalo Databank (UBDB)^{49–51} with the exact potential and multipole method (EPMM).⁵² Among the goals of the present study is the assessment of the performance of this technique in determining the electrostatic energy for Watson–Crick base pairs by comparing the UBDB+EPMM results with the ab initio data.

Computational Details

Geometry of Investigated Complexes and the QTAIM Analysis. The monomers considered in this study were optimized at the MP2/AUG-cc-pVDZ level of theory with C_s symmetry imposed using the GAMESS US package.⁵³ The relative position and orientation of guanine (adenine) and cytosine (thymine) were uniquely defined by the six base-pair parameters (*buckle*, *stagger*, *shear*, *propeller*, *opening*; see Figure 1). These parameters were used for subsequent generation of the complexes with the aid of the 3DNA program⁵⁴ based on the experimentally determined values taken from crystallographic data.⁵⁵ We will refer to such complexes as crystallographic structures.

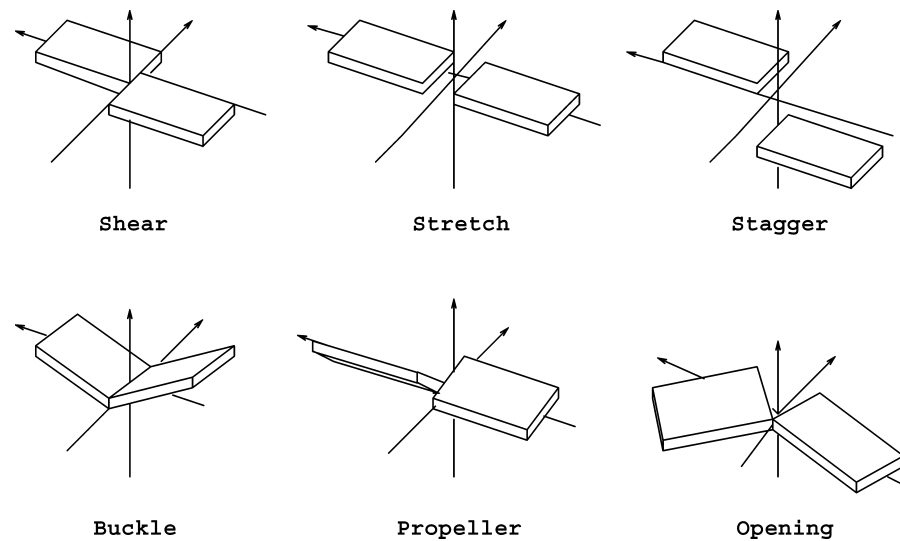


Figure 1. Structural base-pair parameters describing mutual orientation of bases in complexes.

The QTAIM electron density analysis was performed with the AIM2000 package⁵⁶ using the generalized densities obtained at the MP2/AUG-cc-pVDZ level of theoretical approximation.

Intermolecular Interaction Energy Partitioning. In the present work, we adopt a hybrid variational–perturbational approach to evaluate the intermolecular interaction energy components. In this scheme, which retains the physical meaning and clarity of outline of the polarization approximation with the ease of estimation of the exchange effects in a variational approach,^{28,29,57–59} the supermolecular interaction energy calculated with the aid of the second-order Møller–Plesset perturbation theory is partitioned into the Hartree–Fock and Coulomb electron correlation interaction energy components:

$$\Delta E^{\text{MP2}} = \Delta E^{\text{HF}} + \varepsilon_{\text{MP}}^{(2)} \quad (1)$$

The Hartree–Fock interaction energy term can be partitioned into the Heitler–London interaction energy and the $\Delta E_{\text{del}}^{\text{HF}}$ component encompassing collectively the induction and the associated exchange effects due to the Pauli exclusion principle.^{60,61} The former contains the electrostatic interactions of unperturbed monomer charge densities, $\varepsilon_{\text{el}}^{(10)}$, as well as the associated exchange repulsion $\varepsilon_{\text{ex}}^{\text{HL}}$. In terms of symmetry-adapted perturbation theory of intermolecular interactions, the delocalization component encompasses the second- and higher-order induction and exchange-induction terms.⁶²

$$\begin{aligned} \Delta E^{\text{HF}} &= \Delta E_{\text{del}}^{\text{HF}} + \Delta E^{\text{HL}} \\ &= \Delta E_{\text{del}}^{\text{HF}} + \varepsilon_{\text{el}}^{(10)} + \varepsilon_{\text{ex}}^{\text{HL}} \end{aligned} \quad (2)$$

The second-order electron correlation correction term, $\varepsilon_{\text{MP}}^{(2)}$, can be decomposed into the second-order dispersion interaction and the correlation corrections to the Hartree–Fock components:^{28,29}

$$\varepsilon_{\text{MP}}^{(2)} = \varepsilon_{\text{disp}}^{(20)} + \varepsilon_{\text{el,r}}^{(12)} + \Delta E_{\text{ex-del}}^{(2)} \quad (3)$$

The $\varepsilon_{\text{el,r}}^{(12)}$ term is calculated by using the formula proposed by Moszynski et al.,⁶³ whereas $\varepsilon_{\text{el}}^{(10)}$ and $\varepsilon_{\text{disp}}^{(20)}$ components are obtained by standard polarization perturbation theory.⁶⁴ In all necessary calculations the dimer-centered basis set (DCBS) is

used and therefore the results are basis set superposition error (BSSE) free due to the full counterpoise correction.⁶⁵ The detailed outline of the hybrid variational–perturbational interaction energy partitioning scheme and the recent implementation adopted in this work can also be found elsewhere.^{66–68} Since the reorganizations of the electron density of the interacting subsystems occurring at the Heitler–London level of theory are only due to the small rotations of orbitals accompanying their orthogonalization, the visible changes can be attributed almost exclusively to the delocalization interaction energy term. Thus, the interaction difference density (IDD)

$$\Delta\rho(\mathbf{r}) = \rho_{\text{AB}}(\mathbf{r}) - \rho_{\text{A}}(\mathbf{r}) - \rho_{\text{B}}(\mathbf{r}) \quad (4)$$

might be very helpful in the interpretation of the results of interaction energy partitioning, as it allows to visualize the changes in the electron density distributions of monomers occurring upon their interaction. The IDD isodensity maps, presented in this study, were plotted using the electron density matrices obtained by subtraction of the one-particle density matrices of monomers (A, B) from the density matrix of dimer (AB), all corresponding to the respective Hartree–Fock solutions. The interaction difference density maps were plotted using the modified version⁶⁹ of the MOLDEN program.⁷⁰

UBDB/EPMM Method. The UBDB is a data bank of aspherical pseudoatoms derived by Fourier-space fitting of pseudoatoms to molecular electron densities, obtained from ab initio calculations performed at the B3LYP/6-31G(d,p) level of theory.^{49–51} Apart from its application to the refinement of macromolecular X-ray data,⁷¹ the UBDB is designed for the evaluation of the electrostatic properties of large molecular complexes from the reconstituted molecular electron density.^{51,72,73} It has been already shown that in the case of amino acids, the UBDB predicts, with the chemical accuracy, the local and integrated properties of the electron density⁵⁰ and electrostatic interaction energies.⁷⁴ Recently, the databank has been extended by a set of over 50 new atom types with an eye toward calculations of the aspherical atoms' parameters for species present in RNA and DNA molecules. The presence of substituted heteroaromatic rings and the importance of π -interactions for such systems (a phenomenon not present to such extent in amino acids) necessitates a careful testing of the already established algorithm for the atom type definitions. To verify

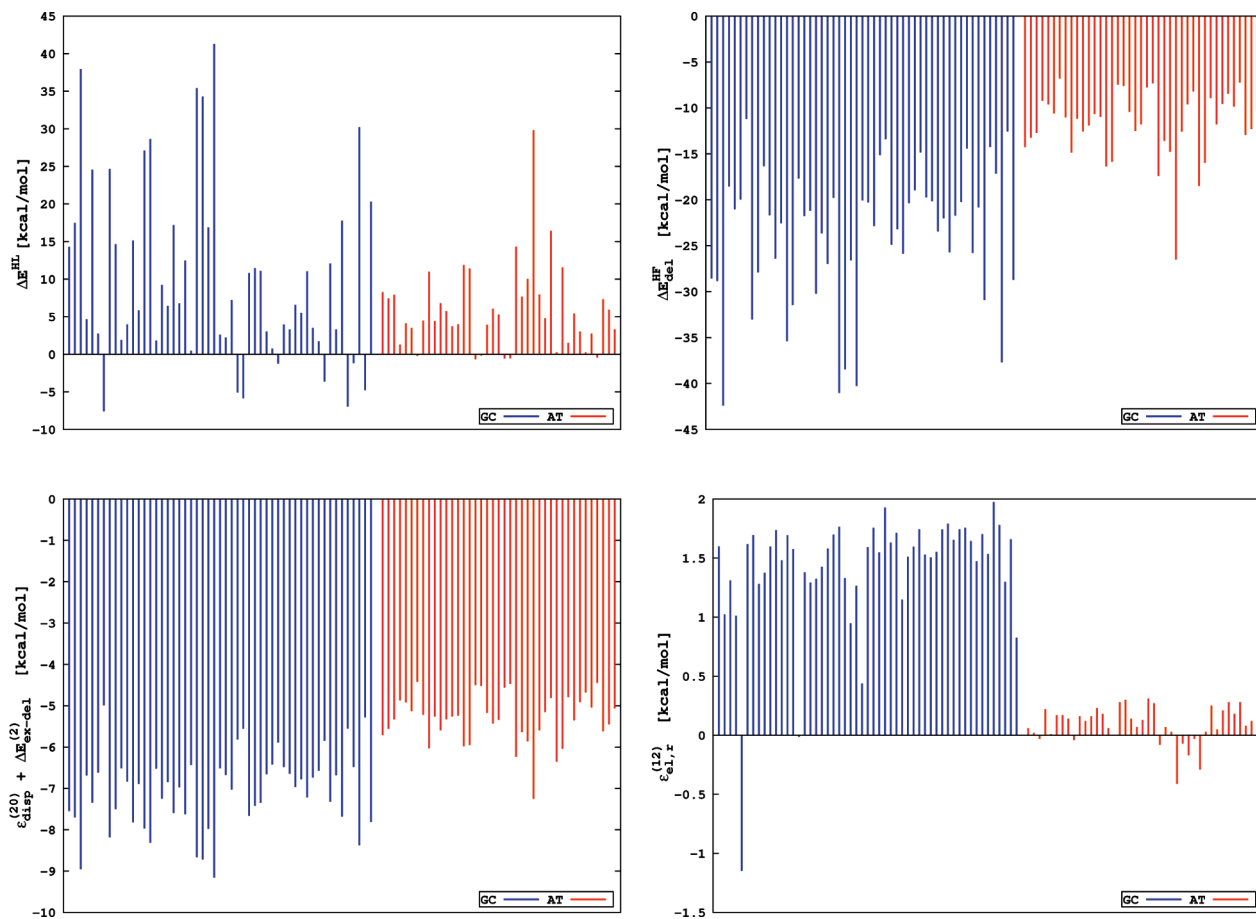


Figure 2. Intermolecular interaction energy components for the crystallographic set of structures.

new atom types and the accuracy of electrostatic energy calculations, the values of electrostatic interaction energy for Watson–Crick adenine–thymine and guanine–cytosine dimers obtained with the UBDB+EPMM method will be compared with the first-order electrostatic interaction energy term, $\epsilon_{el}^{(10)}$. The UBDB databank, together with the LSDB program, was used to reconstruct the electron-density distributions of the NAB complexes. To ensure electroneutrality, all monomers were adjusted *a posteriori* to their net charges by scaling the pseudoatoms according to the Faerman and Price scaling algorithm⁷⁵ implemented in the LSDB. The EPMM method,⁵² implemented in the XDPROP module of the XD2006 package,⁷⁶ was used to calculate electrostatic interactions from reconstructed densities. The method combines numerical evaluation of the exact Coulomb integral in the inner region ($\leq 4.5 \text{ \AA}$) with the Buckingham-type multipole approximation for the long-range interatomic interactions.

Results and Discussion

Structural and Energetic Diversity of Crystallographic Structures of NABs. The calculations were performed for nearly 100 Watson–Crick crystallographic structures. For 53 guanine–cytosine and 40 adenine–thymine complexes the intermolecular interaction energy decomposition was performed. For these complexes, calculations were carried out at the MP2/AUG-cc-pVDZ level of theory. For the structures described by parameters occurring predominantly in the population, i.e., BD0002 (G-C) and BD0037 (A-T) complexes, the intermolecular interaction energies were also determined at the CCSD/AUG-cc-pVDZ level of theory. The differences between the

values of intermolecular interaction energy determined at the MP2 and CCSD levels of theory are equal to -1.38 and 1.27 kcal/mol for the G-C and the A-T pairs, respectively. It is evident that for the H-bonded complexes studied in this work the MP2/AUG-cc-pVDZ level of theory proves to be entirely adequate. As already pointed out,²⁵ even though the dispersion component of interaction energy in terms of magnitude is not negligible, it is of minor importance for H-bonded NAB complexes. Thus, the MP2 level of theory seems to be sufficient to account for electron correlation effects. Furthermore, the MP2 interaction energies calculated with the AUG-cc-pVDZ basis set are very close to the complete basis set (CBS) limit for this type of complexes. In the case of systems considered here, the basis set extension leads to only slightly more negative values of IIEs. For instance, for the representative complexes denoted as BD0002 (G-C) and BD0037 (A-T) the IIEs are equal to -21.9 and -11.7 kcal/mol, while the corresponding differences, when passing from AUG-cc-pVDZ to AUG-cc-pVTZ basis set, amount to -1.94 and -1.18 kcal/mol, i.e., amount to approximately 10% of the calculated values. Further extension of the basis set, from AUG-cc-pVTZ to AUG-cc-pVQZ, increases the respective magnitudes of IIEs only by -0.73 and -0.44 kcal/mol, respectively.

The results of decomposition of interaction energy for the studied crystallographic structures are presented in Figure 2. The structural base-pair parameters for the selected set of crystallographic complexes are presented in the Supporting Information. All the analyzed complexes are stable. In the case of guanine and cytosine complexes, the total intermolecular interaction energy ranges between -7.7 and -24.7 kcal/mol

TABLE 1: Intermolecular Interaction Energy Components for Shear Parameter (in Å) Obtained at the MP2/AUG-cc-pVDZ Level of Theory^a

value	$\epsilon_{\text{el}}^{(10)}$	$\epsilon_{\text{ex}}^{\text{HL}}$	$\Delta E_{\text{del}}^{\text{HF}}$	$\epsilon_{\text{el,r}}^{(12)}$	$\epsilon_{\text{disp}}^{(20)}$	$\Delta E_{\text{ex-del}}^{(2)}$	$\epsilon_{\text{MP}}^{(2)}$	ΔE^{HL}	ΔE^{HF}	ΔE^{MP2}
G-C										
-0.69	-36.00	33.31	-15.26	1.62	-13.49	7.62	-4.25	-2.68	-17.94	-22.19
-0.54	-40.65	41.10	-18.23	1.70	-14.91	8.60	-4.62	0.45	-17.78	-22.40
-0.39	-45.19	49.34	-21.29	1.72	-16.34	9.62	-5.01	4.15	-17.14	-22.15
-0.23	-49.19	57.37	-24.14	1.64	-17.72	10.63	-5.45	8.18	-15.97	-21.41
-0.08	-52.10	64.17	-26.30	1.45	-18.92	11.55	-5.92	12.06	-14.23	-20.15
0.08	-53.56	69.13	-27.52	1.12	-19.92	12.35	-6.45	15.57	-11.95	-18.40
0.23	-53.19	71.40	-27.44	0.65	-20.60	12.94	-7.01	18.21	-9.23	-16.24
0.39	-51.03	71.36	-26.32	0.05	-21.04	13.37	-7.61	20.32	-6.00	-13.61
0.54	-47.40	69.64	-24.48	-0.61	-21.32	13.69	-8.24	22.24	-2.24	-10.48
0.69	-42.69	67.35	-22.46	-1.29	-21.52	13.93	-8.89	24.66	2.20	-6.68
A-T										
-0.34	-24.73	28.54	-10.28	0.01	-10.93	5.87	-5.05	3.82	-6.46	-11.52
-0.26	-25.73	29.84	-10.83	0.07	-11.15	6.01	-5.07	4.11	-6.72	-11.79
-0.18	-26.46	30.94	-11.26	0.11	-11.33	6.13	-5.09	4.49	-6.78	-11.87
-0.10	-26.96	31.73	-11.59	0.14	-11.50	6.22	-5.14	4.78	-6.82	-11.95
-0.02	-27.15	32.23	-11.77	0.14	-11.61	6.29	-5.18	5.08	-6.68	-11.86
0.06	-27.04	32.45	-11.78	0.11	-11.69	6.34	-5.24	5.40	-6.37	-11.60
0.14	-26.68	32.33	-11.66	0.07	-11.73	6.36	-5.30	5.66	-6.00	-11.30
0.22	-26.05	31.92	-11.39	-0.01	-11.72	6.36	-5.36	5.87	-5.52	-10.89
0.30	-25.19	31.24	-11.03	-0.10	-11.68	6.34	-5.44	6.04	-4.99	-10.43
0.38	-24.09	30.31	-10.53	-0.22	-11.61	6.30	-5.53	6.21	-4.32	-9.85

^a All energies are given in kcal/mol.**TABLE 2:** Intermolecular Interaction Energy Components for Stretch Parameter (in Å) Obtained at the MP2/AUG-cc-pVDZ Level of Theory^a

value	$\epsilon_{\text{el}}^{(10)}$	$\epsilon_{\text{ex}}^{\text{HL}}$	$\Delta E_{\text{del}}^{\text{HF}}$	$\epsilon_{\text{el,r}}^{(12)}$	$\epsilon_{\text{disp}}^{(20)}$	$\Delta E_{\text{ex-del}}^{(2)}$	$\epsilon_{\text{MP}}^{(2)}$	ΔE^{HL}	ΔE^{HF}	ΔE^{MP2}
G-C										
-0.36	-64.37	95.49	-37.43	1.29	-24.32	15.77	-7.26	31.12	-6.31	-13.57
-0.29	-57.61	78.10	-31.37	1.44	-21.47	13.54	-6.49	20.50	-10.87	-17.37
-0.23	-51.71	63.75	-26.37	1.58	-18.97	11.60	-5.79	12.04	-14.33	-20.12
-0.17	-46.67	52.10	-22.31	1.71	-16.81	9.95	-5.14	5.44	-16.87	-22.02
-0.11	-42.17	42.47	-18.88	1.80	-14.89	8.51	-4.57	0.29	-18.59	-23.16
-0.04	-38.30	34.66	-16.08	1.87	-13.22	7.29	-4.06	-3.65	-19.73	-23.80
0.02	-34.92	28.23	-13.74	1.93	-11.75	6.22	-3.60	-6.70	-20.44	-24.03
0.08	-31.97	22.97	-11.77	1.97	-10.45	5.31	-3.17	-9.00	-20.77	-23.94
0.14	-29.35	18.69	-10.13	2.00	-9.32	4.53	-2.80	-10.66	-20.79	-23.59
0.20	-27.05	15.19	-8.75	2.01	-8.32	3.85	-2.46	-11.86	-20.61	-23.07
A-T										
-0.36	-46.17	76.37	-26.93	-0.30	-19.56	12.30	-7.56	30.19	3.26	-4.30
-0.31	-41.77	65.39	-23.09	-0.21	-17.76	10.89	-7.07	23.55	0.46	-6.61
-0.27	-37.86	55.97	-19.84	-0.12	-16.15	9.66	-6.62	18.11	-1.73	-8.35
-0.22	-34.40	47.96	-17.10	-0.04	-14.71	8.57	-6.18	13.56	-3.54	-9.76
-0.17	-31.30	41.10	-14.77	0.03	-13.42	7.61	-5.78	9.79	-5.78	-10.75
-0.13	-28.49	35.13	-12.74	0.90	-12.23	6.74	-5.40	6.64	-6.09	-11.49
-0.08	-25.95	30.06	-10.98	0.15	-11.16	5.96	-5.04	4.11	-6.87	-11.92
-0.03	-23.75	25.78	-9.55	0.21	-10.22	5.29	-4.72	2.03	-7.51	-12.23
0.01	-21.75	22.11	-8.28	0.25	-9.36	4.70	-4.41	0.36	-7.92	-12.33
0.06	-19.88	18.83	-7.15	0.29	-8.55	4.14	-4.11	-1.06	-8.21	-12.32

^a All energies are given in kcal/mol.

while for adenine-thymine complexes the values of total intermolecular interaction energy are between -4.4 and -12.6 kcal/mol. Therefore, the apparently larger structural diversity observed for G-C complexes is reflected in the larger anisotropy of the relative changes of the total IIEs. In most of the studied systems the first-order electrostatic term is the largest stabilizing component in terms of magnitude. However, after considering the associated exchange repulsion, the net effect of the two terms, i.e., ΔE^{HL} , is repulsive for the vast majority of the considered structures. Even though the absolute value of the first-order electrostatic energy is larger than the HL exchange energy for certain G-C complexes (BD0032, BD0002, BD0047), still the delocalization component is much larger than the HL term. The analyzed Watson-Crick structures are further stabilized by the dispersion energy, as previously reported by Toczyłowski and Cybulski²⁵ and later by Hesselman et al.²³ The dispersion contribution in the studied complexes is indeed substantial. Its mean values exceed -11 and -17 kcal/mol for the studied A-T and G-C complexes, respectively. However, it is significantly damped by the exchange-correlation effects which respective mean values exceed +6 and +10 kcal/mol.

Directionality of Interactions and Approximate Potentials. In order to analyze the dependence of the intermolecular interaction energy components on changes of geometrical parameters, two structures described by the values of parameters occurring predominantly were selected: BD0002 for G-C and BD0037 for A-T. For these structures the potential energy surface scans with respect to a given base-pair parameter, with

TABLE 3: Intermolecular Interaction Energy Components for Stagger Parameter (in Å) Obtained at the MP2/AUG-cc-pVDZ Level of Theory^a

value	$\epsilon_{\text{el}}^{(10)}$	$\epsilon_{\text{ex}}^{\text{HL}}$	$\Delta E_{\text{del}}^{\text{HF}}$	$\epsilon_{\text{el,r}}^{(12)}$	$\epsilon_{\text{disp}}^{(20)}$	$\Delta E_{\text{ex-del}}^{(2)}$	$\epsilon_{\text{MP}}^{(2)}$	ΔE^{HL}	ΔE^{HF}	ΔE^{MP2}
G-C										
-0.63	-38.62	40.10	-17.28	1.74	-14.48	8.09	-4.65	1.48	-15.79	-20.44
-0.48	-42.11	45.46	-19.50	1.71	-15.53	8.92	-4.89	3.35	-16.15	-21.05
-0.33	-45.00	49.83	-21.32	1.70	-16.37	9.60	-5.07	4.82	-16.50	-21.56
-0.18	-47.09	52.96	-22.62	1.70	-16.97	10.07	-5.19	5.87	-16.75	-21.94
-0.04	-48.25	54.62	-23.28	1.69	-17.30	10.33	-5.27	6.37	-16.91	-22.18
0.11	-48.26	54.41	-23.12	1.70	-17.29	10.32	-5.27	6.15	-16.97	-22.24
0.26	-47.27	52.57	-22.31	1.72	-16.99	10.06	-5.20	5.30	-17.01	-22.21
0.41	-45.28	49.26	-20.87	1.74	-16.42	9.58	-5.09	3.98	-16.88	-21.97
0.55	-42.54	44.82	-19.02	1.77	-15.60	8.92	-4.91	2.28	-16.74	-21.64
0.70	-39.21	39.57	-16.83	1.80	-14.58	8.12	-4.66	0.36	-16.47	-21.13
A-T										
-0.56	-22.54	24.71	-8.70	0.23	-10.16	5.16	-4.77	2.17	-6.53	-11.30
-0.46	-23.86	26.79	-9.49	0.20	-10.59	5.48	-4.91	2.92	-6.57	-11.48
-0.35	-25.07	28.66	-10.26	0.18	-10.97	5.77	-5.02	3.59	-6.67	-11.69
-0.25	-25.98	30.17	-10.87	0.15	-11.26	6.00	-5.11	4.19	-6.68	-11.79
-0.14	-26.70	31.41	-11.39	0.14	-11.49	6.18	-5.17	4.71	-6.69	-11.86
-0.04	-27.07	32.09	-11.67	0.13	-11.61	6.28	-5.19	5.02	-6.65	-11.84
0.07	-27.13	32.40	-11.79	0.13	-11.66	6.32	-5.21	5.27	-6.52	-11.73
0.17	-26.90	32.17	-11.71	0.13	-11.61	6.29	-5.19	5.27	-6.44	-11.64
0.28	-26.27	31.38	-11.37	0.14	-11.45	6.16	-5.15	5.11	-6.26	-11.42
0.39	-25.37	30.18	-10.85	0.14	-11.21	5.98	-5.09	4.82	-6.04	-11.13

^a All energies are given in kcal/mol.

TABLE 4: Intermolecular Interaction Energy Components for Buckle Parameter (in degrees) Obtained at the MP2/AUG-cc-pVDZ Level of Theory^a

value	$\epsilon_{\text{el}}^{(10)}$	$\epsilon_{\text{ex}}^{\text{HL}}$	$\Delta E_{\text{del}}^{\text{HF}}$	$\epsilon_{\text{el,r}}^{(12)}$	$\epsilon_{\text{disp}}^{(20)}$	$\Delta E_{\text{ex-del}}^{(2)}$	$\epsilon_{\text{MP}}^{(2)}$	ΔE^{HL}	ΔE^{HF}	ΔE^{MP2}
G-C										
-19.39	-52.87	64.56	-26.40	1.63	-19.19	11.65	-5.91	11.70	-14.71	-20.62
-15.97	-51.86	62.04	-25.77	1.68	-18.70	11.29	-5.72	10.18	-15.59	-21.31
-12.55	-50.89	59.71	-25.12	1.74	-18.25	10.97	-5.54	8.82	-16.31	-21.85
-9.13	-49.82	57.57	-24.45	1.75	-17.84	10.67	-5.42	7.75	-16.70	-22.12
-5.70	-48.67	55.46	-23.68	1.75	-17.44	10.40	-5.30	6.79	-16.88	-22.18
-2.28	-47.43	53.45	-22.85	1.72	-17.06	10.13	-5.21	6.02	-16.82	-22.06
1.14	-46.19	51.71	-22.05	1.66	-16.73	9.91	-5.16	5.52	-16.53	-21.68
4.56	-44.98	50.06	-21.26	1.61	-16.42	9.70	-5.11	5.08	-16.18	-21.29
7.98	-43.75	48.70	-20.51	1.53	-16.16	9.54	-5.10	4.94	-15.56	-20.66
11.40	-42.64	47.62	-19.83	1.45	-15.96	9.41	-5.09	4.98	-14.85	-19.98
A-T										
-7.24	-26.68	32.33	-11.58	0.06	-11.67	6.35	-5.26	5.65	-5.92	-11.18
-5.41	-26.74	32.23	-11.59	0.07	-11.64	6.34	-5.23	5.49	-6.09	-11.33
-3.57	-26.79	32.18	-11.61	0.08	-11.62	6.32	-5.22	5.39	-6.22	-11.44
-1.74	-26.87	32.17	-11.65	0.10	-11.62	6.31	-5.21	5.30	-6.35	-11.55
0.09	-26.94	32.21	-11.68	0.10	-11.62	6.31	-5.20	5.27	-6.41	-11.61
1.93	-27.05	32.28	-11.75	0.12	-11.64	6.31	-5.20	5.22	-6.52	-11.73
3.76	-27.16	32.43	-11.82	0.13	-11.67	6.33	-5.21	5.26	-6.56	-11.77
5.59	-27.22	32.48	-11.85	0.14	-11.68	6.33	-5.22	5.26	-6.59	-11.80
7.43	-27.38	32.74	-11.96	0.15	-11.74	6.35	-5.24	5.36	-6.61	-11.84
9.26	-27.50	32.93	-12.04	0.16	-11.79	6.37	-5.26	5.43	-6.61	-11.87

^a All energies are given in kcal/mol.

the remaining five kept fixed, were performed. The ranges of variability of the scanned base-pair parameters were chosen based on the experimental data and were divided into 10 equal intervals for which the interaction energy decomposition was performed. It should be underscored that the previously discussed crystallographic set and the set used for scanning contain slightly different structures, even though the configurational space is spanned over the same range of parameters. Nevertheless, the range of variability of IIEs is quite similar and in the case of G-C it spans the range from -6.7 to -24.0 kcal/mol while for A-T complexes it ranges from -4.3 to -12.4 kcal/mol. Furthermore, such an approach provides grounds for a more systematic analysis of the dependencies of interaction

energy components on the selected structural parameters. The complete sets of results are presented in Tables 1–6 whereas in Figures 3–5 the selected IIE components are plotted against the structural parameters. The most striking feature observed in the plots is the generally significantly smaller anisotropy of interactions for A-T complexes in comparison with G-C base pairs. In fact, only the scan with respect to the stretch parameter leads to the similar relative changes of the interaction energy terms for both complexes. In the case of the remaining parameters, the respective relative changes of the A-T interaction energies and its components are much smaller than those revealed for the G-C complexes. Generally, the observed variations of interaction energy components are much more

TABLE 5: Intermolecular Interaction Energy Components for Propeller Parameter (in degrees) Obtained at the MP2/AUG-cc-pVDZ Level of Theory^a

value	$\epsilon_{\text{el}}^{(10)}$	$\epsilon_{\text{ex}}^{\text{HL}}$	$\Delta E_{\text{del}}^{\text{HF}}$	$\epsilon_{\text{el,r}}^{(12)}$	$\epsilon_{\text{disp}}^{(20)}$	$\Delta E_{\text{ex-del}}^{(2)}$	$\epsilon_{\text{MP}}^{(2)}$	ΔE^{HL}	ΔE^{HF}	ΔE^{MP2}
G-C										
-20.12	-40.81	44.28	-19.09	1.57	-15.30	8.72	-5.00	3.47	-15.62	-20.63
-17.01	-42.72	46.82	-20.14	1.62	-15.80	9.13	-5.06	4.10	-16.04	-21.10
-13.91	-44.48	49.25	-21.13	1.66	-16.27	9.51	-5.11	4.77	-16.37	-21.48
-10.80	-46.06	51.45	-22.03	1.69	-16.69	9.85	-5.15	5.39	-16.63	-21.79
-7.69	-47.40	53.45	-22.80	1.70	-17.05	10.15	-5.21	6.04	-16.76	-21.97
-4.59	-48.55	54.99	-23.46	1.73	-17.34	10.39	-5.22	6.44	-17.01	-22.24
-1.48	-49.11	55.85	-23.75	1.72	-17.49	10.52	-5.25	6.74	-17.01	-22.26
1.63	-49.22	55.97	-23.76	1.71	-17.53	10.54	-5.27	6.76	-17.00	-22.27
4.73	-48.91	55.38	-23.49	1.72	-17.44	10.47	-5.26	6.46	-17.03	-22.29
7.84	-48.03	53.96	-22.89	1.69	-17.22	10.27	-5.25	5.93	-16.95	-22.21
A-T										
-17.76	-26.69	31.88	-11.59	0.11	-11.54	6.24	-5.19	5.19	-6.40	-11.59
-15.38	-27.24	32.49	-11.85	0.13	-11.68	6.34	-5.21	5.26	-6.59	-11.80
-13.00	-27.67	32.96	-12.02	0.14	-11.79	6.42	-5.22	5.29	-6.73	-11.95
-10.63	-28.10	33.43	-12.22	0.15	-11.89	6.50	-5.24	5.33	-6.89	-12.12
-8.25	-28.39	33.76	-12.33	0.16	-11.97	6.57	-5.25	5.37	-6.96	-12.21
-5.87	-28.69	34.12	-12.47	0.16	-12.05	6.63	-5.26	5.44	-7.03	-12.30
-3.50	-28.84	34.30	-12.53	0.16	-12.09	6.66	-5.28	5.47	-7.06	-12.34
-1.12	-28.94	34.40	-12.57	0.16	-12.11	6.68	-5.27	5.46	-7.11	-12.38
1.26	-28.89	34.36	-12.57	0.15	-12.11	6.67	-5.28	5.46	-7.07	-12.35
3.63	-28.80	34.23	-12.48	0.15	-12.08	6.66	-5.27	5.43	-7.04	-12.32

^a All energies are given in kcal/mol.

TABLE 6: Intermolecular Interaction Energy Components for Opening Parameter (in degrees) Obtained at the MP2/AUG-cc-pVDZ Level of Theory^a

value	$\epsilon_{\text{el}}^{(10)}$	$\epsilon_{\text{ex}}^{\text{HL}}$	$\Delta E_{\text{del}}^{\text{HF}}$	$\epsilon_{\text{el,r}}^{(12)}$	$\epsilon_{\text{disp}}^{(20)}$	$\Delta E_{\text{ex-del}}^{(2)}$	$\epsilon_{\text{MP}}^{(2)}$	ΔE^{HL}	ΔE^{HF}	ΔE^{MP2}
G-C										
-5.60	-46.20	55.08	-23.52	1.71	-16.44	9.89	-4.83	8.89	-14.63	-19.46
-4.10	-45.92	52.92	-22.76	1.72	-16.36	9.76	-4.88	7.00	-15.76	-20.64
-2.61	-46.01	51.78	-22.37	1.73	-16.41	9.73	-4.94	5.77	-16.60	-21.54
-1.12	-46.29	51.79	-22.26	1.71	-16.62	9.84	-5.07	5.49	-16.77	-21.84
0.37	-47.13	53.12	-22.64	1.69	-17.02	10.11	-5.22	5.99	-16.65	-21.87
1.86	-48.25	55.67	-23.31	1.65	-17.58	10.50	-5.42	7.42	-15.88	-21.31
3.36	-49.92	59.80	-24.46	1.61	-18.33	11.06	-5.66	9.88	-14.58	-20.24
4.85	-52.19	65.94	-26.21	1.55	-19.34	11.83	-5.96	13.76	-12.45	-18.41
6.34	-55.04	74.37	-28.59	1.47	-20.60	12.81	-6.32	19.33	-9.26	-15.58
7.83	-58.67	85.52	-31.77	1.38	-22.14	14.03	-6.72	26.85	-4.92	-11.64
A-T										
-7.02	-29.25	37.72	-13.27	-0.09	-12.45	6.98	-5.57	8.47	-4.80	-10.37
-5.52	-28.62	35.83	-12.75	-0.03	-12.17	6.75	-5.45	7.22	-5.53	-10.98
-4.02	-28.05	34.31	-12.30	0.01	-11.93	6.56	-5.36	6.26	-6.04	-11.40
-2.52	-27.67	33.31	-12.03	0.04	-11.78	6.44	-5.29	5.64	-6.39	-11.69
-1.02	-27.35	32.57	-11.81	0.08	-11.66	6.34	-5.24	5.21	-6.60	-11.84
0.47	-27.18	32.25	-11.73	0.10	-11.61	6.30	-5.21	5.07	-6.66	-11.87
1.97	-27.13	32.24	-11.74	0.12	-11.63	6.30	-5.20	5.11	-6.63	-11.83
3.47	-27.15	32.52	-11.83	0.13	-11.69	6.34	-5.21	5.38	-6.45	-11.66
4.97	-27.24	33.05	-11.98	0.13	-11.80	6.44	-5.24	5.81	-6.17	-11.41
6.46	-27.43	33.85	-12.21	0.13	-11.96	6.54	-5.28	6.43	-5.79	-11.07

^a All energies are given in kcal/mol.

pronounced for the translational parameters, particularly for stretch parameter, for which the relative changes of the total interaction energy exceed 40% for border points of both A-T and G-C complexes. Significant changes of the total interaction energy are revealed also in the case of shear parameter for G-C complex, for which the total interaction energy ranges from -6.68 to -22.4 kcal/mol. Although in the case of stagger parameter a significant anisotropy is observed for the individual interaction energy components, the net effect is generally not so evident as in the case of the former two. The only angular parameter for which significant variations of corresponding IIE are observed is opening. These observations seem to contradict some of the previous conclusions of Toczyłowski and Cybulski

who emphasized the strong angular dependence of IIE components.²⁵ We consider two possible reasons for this discrepancy. First, this is most likely due to a slightly different approach to probing the IIE surface, which in our case is based on the standard reference frame used for the description of nucleic acid base-pair geometry, whereas in the aforementioned study it was somewhat arbitrary. Second, the two geometrical parameters used by Toczyłowski and Cybulski are closely connected with stretch and opening; however, they considered much narrower range of variability of these parameters. As it follows from Tables 2 and 6, the change of IIE upon modification of geometrical parameters depends significantly on the region of configurational space. Finally, let us underline that we observe

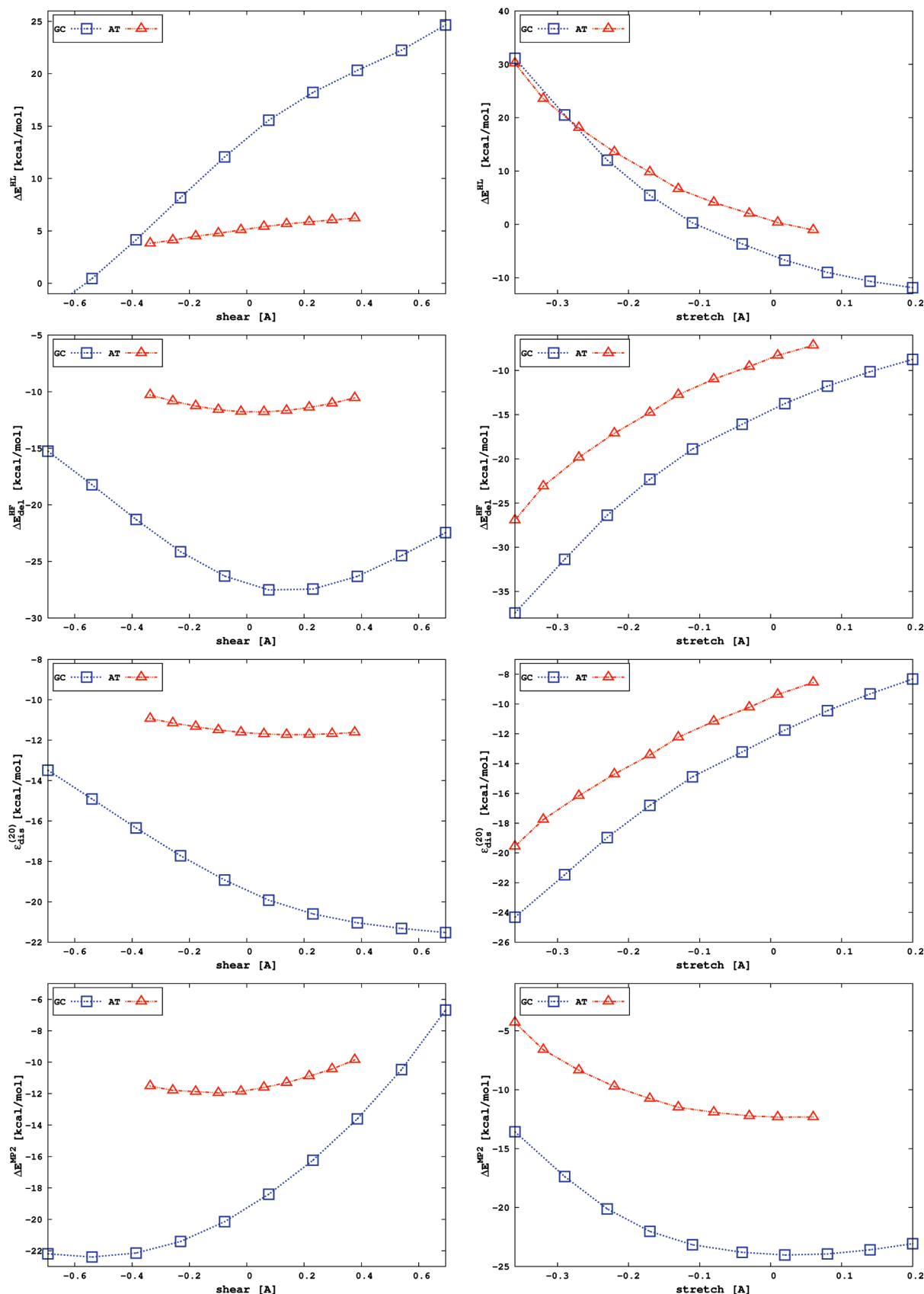


Figure 3. Intermolecular interaction energy components for shear and stretch parameters.

a significant directionality of interactions also for the opening parameter, particularly for the G-C complexes. The same is true for some of the IIE components in the case of propeller and buckle parameters. Nevertheless, the overall effect for both A-T

and G-C complexes results in generally insignificant directionality of interactions for these two parameters. Analysis of the IIE components reveals that the first-order components, i.e., electrostatic and exchange, are characterized by usually much

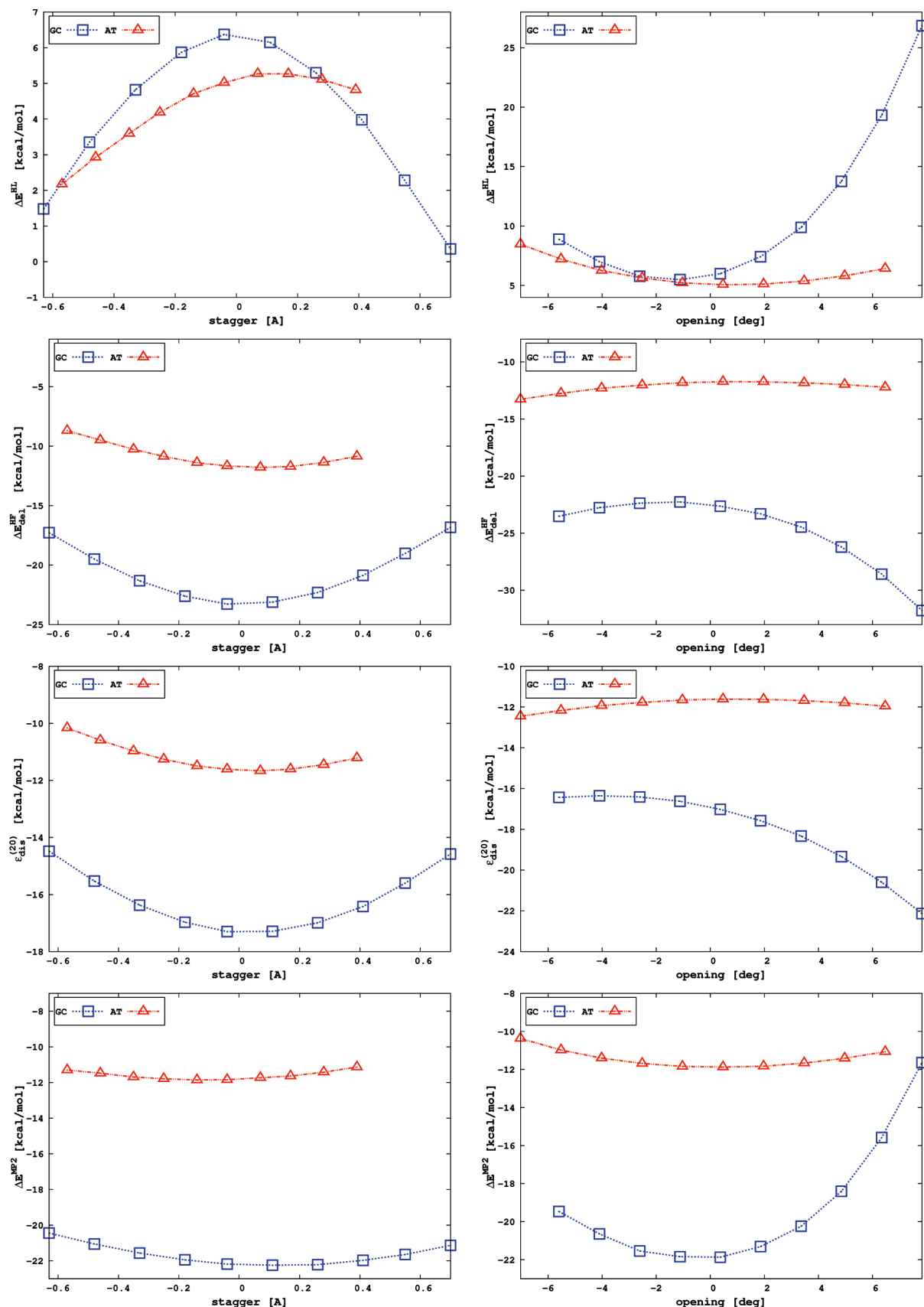


Figure 4. Intermolecular interaction energy components for stagger and opening parameters.

larger anisotropy than the higher-order terms. This observation remains valid for the ΔE^{HL} . Consistent with the observations made for previously discussed crystallographic set, the total Heitler-London interaction energy remains repulsive in almost

all probed regions of the configurational space. In fact, only for the increasing values of stretch parameter, greater than -0.04 \AA in the case of G-C and 0.06 \AA in the case of A-T complex as well as the negative border range of shear for the G-C complex,

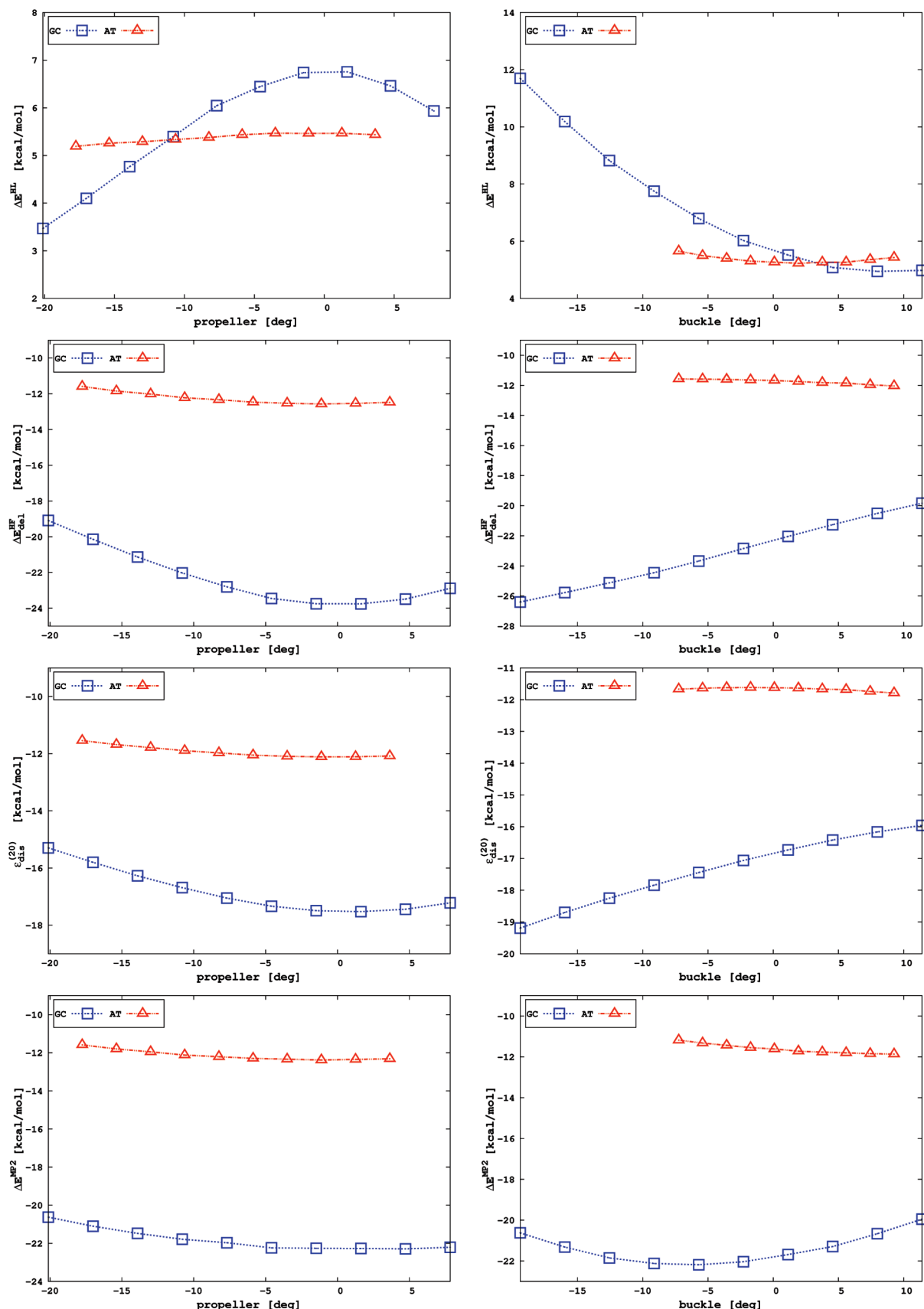


Figure 5. Intermolecular interaction energy components for propeller and buckle parameters.

the electrostatic attraction of the unperturbed monomer charge densities is larger than the associated exchange repulsion. Analysis of the structural parameters of the few G-C complexes from the crystallographic set for which ΔE^{HL} contribution is

also stabilizing reveals that they are characterized by small values of shear parameter and relatively large values of stretch parameter. Although the stabilization due to delocalization component is usually approximately 2 times smaller than the

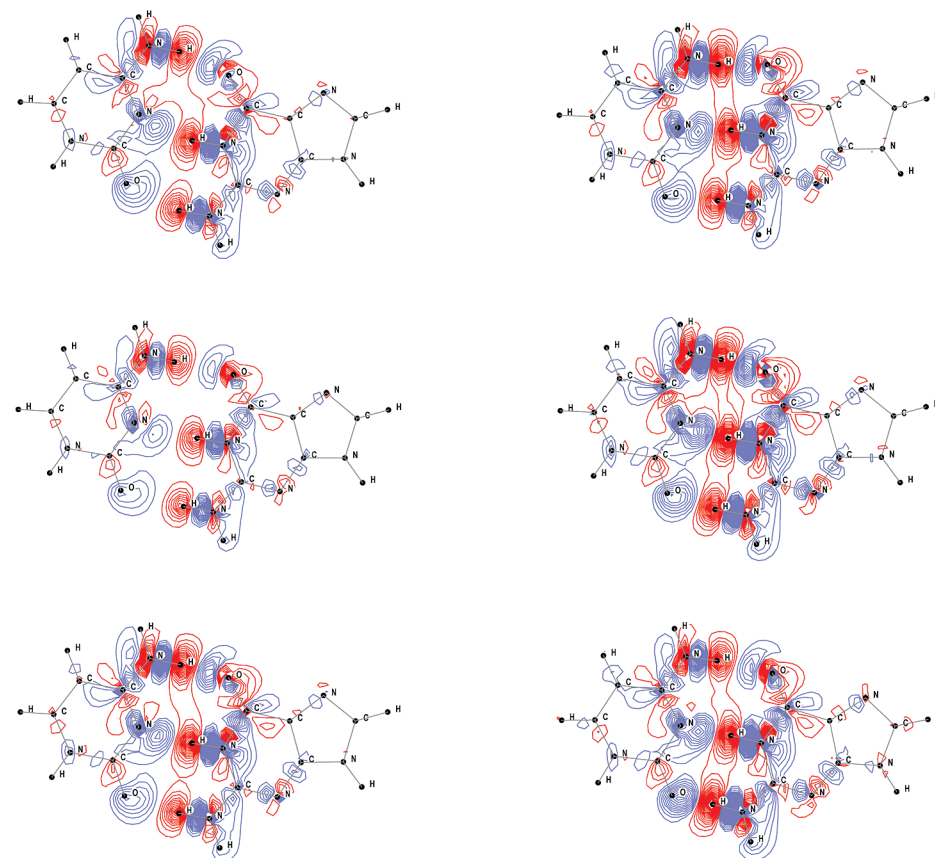


Figure 6. Difference electron density maps for the G-C complex labeled as BD0002 scanned with respect to shear (top), stretch (middle), and stagger (bottom). Red and blue contour lines correspond to negative and positive changes of electron density, respectively. See text for more details.

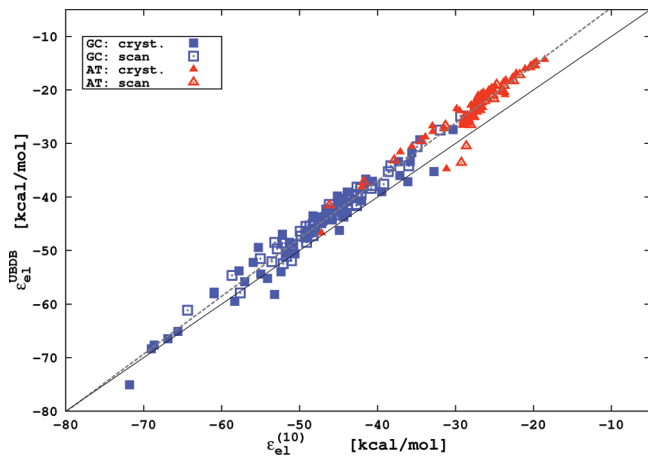


Figure 7. Comparison of electrostatic interaction energy calculated with the UBDB+EPMM method, $\epsilon_{el}^{(UBDB)}$, and using the ab initio methods, $\epsilon_{el}^{(10)}$, for the set of all structures considered in the present study. See text for more details.

electrostatic term, it should be emphasized that ΔE_{del}^{HF} quantifies the effects of mutual polarization of monomer charge densities and the associated Pauli repulsion. Therefore, it is more appropriate to compare this term with the ΔE^{HL} rather than with the $\epsilon_{el}^{(10)}$.

Interestingly, in the case of G-C complexes, the delocalization component assumes its minimum, i.e., a seemingly optimal magnitude, for the values of shear, stagger, and propeller parameters close to zero. On the contrary, the respective repulsion due to ΔE^{HL} term retains its maximum for stagger and propeller parameters and is quite substantial for shear

parameter. Although a similar observation can be made for A-T complexes, these effects are much less pronounced due to a generally weaker dependence of the IIE components on the analyzed structural parameters. In the case of opening parameter, the interaction energy components exhibit the opposite tendencies than those revealed in the case of stagger and propeller parameters. Nevertheless, such a behavior of the delocalization component could indicate at least partially resonance-assistant character of the hydrogen bonds.^{77,78} The dispersion component remains an important stabilizing factor in the whole range of investigated structural parameters, even though it is significantly balanced by the exchange-correlation effects. In the case of stagger, opening, propeller, and buckle parameters, it follows quantitatively the same trends as the delocalization term. However, in the case of the increasing values of shear and the decreasing values of stretch parameters, it becomes particularly important: first, because its magnitude grows significantly and second because the corresponding values of ΔE^{HL} and ΔE_{del}^{HF} components almost completely cancel each other out. This is exceedingly obvious for the values of shear larger than 0.39 Å in the case of G-C complexes and 0.30 Å in the case of A-T, for which the correlation correction to the interaction energy becomes the main origin of stabilization. Similar effects are observed for the values of stretch smaller than -0.36 and -0.17 Å for G-C and A-T complexes, respectively. This observation can be particularly important for development of parametrization of approximate methods of determining the potential energy surfaces in large polynucleotide fragments.

For the three translational parameters, namely shear, stretch, and stagger, for which a relatively strong dependence of the delocalization term was observed, we plotted the difference

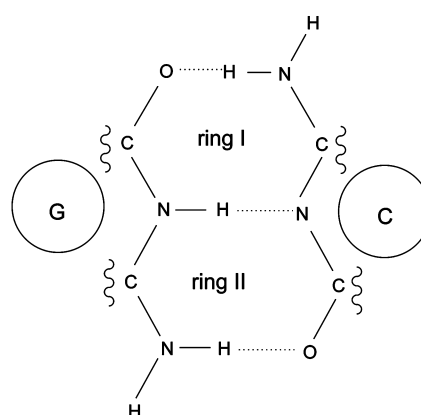
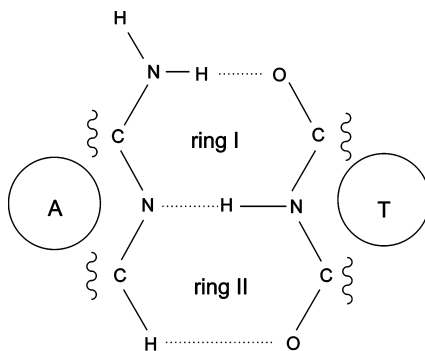


Figure 8. Labeling of hydrogen bonds used throughout this study.

electron density maps for the G-C complex (see Figure 6). The structures on the left and on the right correspond to infima and suprema on the $\Delta E_{\text{del}}^{\text{HF}}$ curves (Figures 3 and 4), respectively. Despite rather large differences in the absolute values of the delocalization component, the qualitative changes of the electron density upon the formation of the complex are quite similar in all three cases and are localized within the moiety involving hydrogen bonds. The visual changes of electron density are the largest for the stretch parameter. This is not surprising as the difference between the stationary points on the $\Delta E_{\text{del}}^{\text{HF}}$ curve is almost 30 kcal/mol.

Figure 7 presents a comparison between the electrostatic energy values calculated using the UBDB+EPMM method and the first-order electrostatic interaction energies for the examined set of A-T and G-C complexes, where index “cryst” refers to crystallographic geometries, while “scan” refers to geometries obtained with the aid of scanning procedure. It should be underlined that both sets comprise the structures described in preceding paragraphs. The correlation between the combined UBDB+EPMM approach and the ab initio data is quite rewarding ($r = 0.991$), and the linear coefficient describing the trend line (marked with dashes in the plot) is close to unity (1.08(1)). The solid line represents a perfect linear correlation. The rms difference between values of $\epsilon_{\text{el}}^{(10)}$ and the UBDB+EPMM results is 3.7 kcal/mol for the set comprising more than 200 Watson–Crick base pairs. Even though Figure 7 clearly shows that the UBDB+EPMM method tends to underestimate the interaction energy when compared to the ab initio results, the overall performance of the UBDB databank is quite satisfactory in predicting electrostatic energy of hydrogen-bonded nucleic acid–base complexes. It should be emphasized here that the UBDB+EPMM method preserves the general tendencies in electrostatic interaction energy values in relation to the structural variety of analyzed complexes. The differences between electrostatic energy values obtained from ab initio calculations and the UBDB+EPMM approach may be partially explained by the different basis sets used in both methods, i.e., AUG-cc-pVDZ and 6-31G(d,p), respectively.

Topological Analysis of Electron Density. In order to gain an insight into the local nature of interactions in hydrogen-bonded Watson–Crick pairs, we carried out an analysis of topological properties of the electronic charge density distributions of the studied complexes within the framework of the QTAIM.^{40,79} Let us briefly review the most relevant features of this approach.

Koch and Popelier developed a set of criteria for determining hydrogen bonds.⁸⁰ Among the key parameters characterizing hydrogen bonds, one finds the magnitude of electron density at

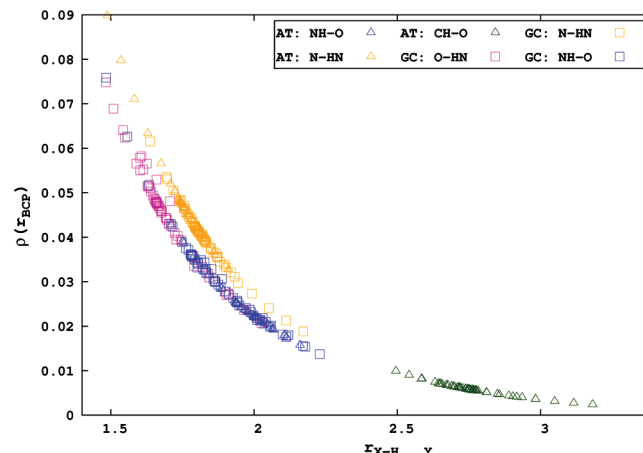


Figure 9. Dependence of $\rho(\mathbf{r})$ at $\text{X}-\text{H}\cdots\text{Y}$ bond critical point on the bond distance.

bond critical points (BCPs), which are the minima of the electron density along the bond path. The other various characteristics of BCP proposed by Bader, particularly the Laplacian of electron density, the electronic kinetic energy density, $G(\mathbf{r})$ and the electronic potential energy density, $V(\mathbf{r})$, are also very helpful in analysis of specific types of interactions such as the closed-shell interactions (ionic bonds, van der Waals interactions, and hydrogen bonds) and shared interactions (i.e., covalent bonds). These parameters allow to classify and characterize the interactions. For instance, interesting correlations have been found for closed-shell interactions between geometrical, energetic, and topological parameters.^{81–86}

The analysis of topological properties of electron density was carried out for the same set of structures that was used for analyzing the anisotropy of interactions. In Figure 8 we define the labeling of hydrogen bonds in the A-T and the G-C base pairs that shall be adopted hereafter. Since our primary interest was to analyze the dependence of the H-bond properties on structural parameters in a systematic manner, we have not attempted to analyze the set of crystallographic structures.

It is quite well established that the electron density $\rho(\mathbf{r})$ at the bond critical point is a good measure of hydrogen bond strength. The shorter the distance $\text{H}\cdots\text{Y}$, the stronger the $\text{XH}\cdots\text{Y}$ hydrogen bond and the greater is the electron density at the corresponding $\text{XH}\cdots\text{Y}$ BCP.⁸² Figure 9 shows the dependence of the electron density at the BCPs on the $\text{XH}\cdots\text{Y}$ distance for all investigated structures of A-T and G-C base pairs. Interestingly, the dependencies of $\rho(\mathbf{r})$ on A-T N \cdots HN and G-C NH \cdots N hydrogen bond lengths follow the same pattern in both cases. It might suggest their similar nature. The

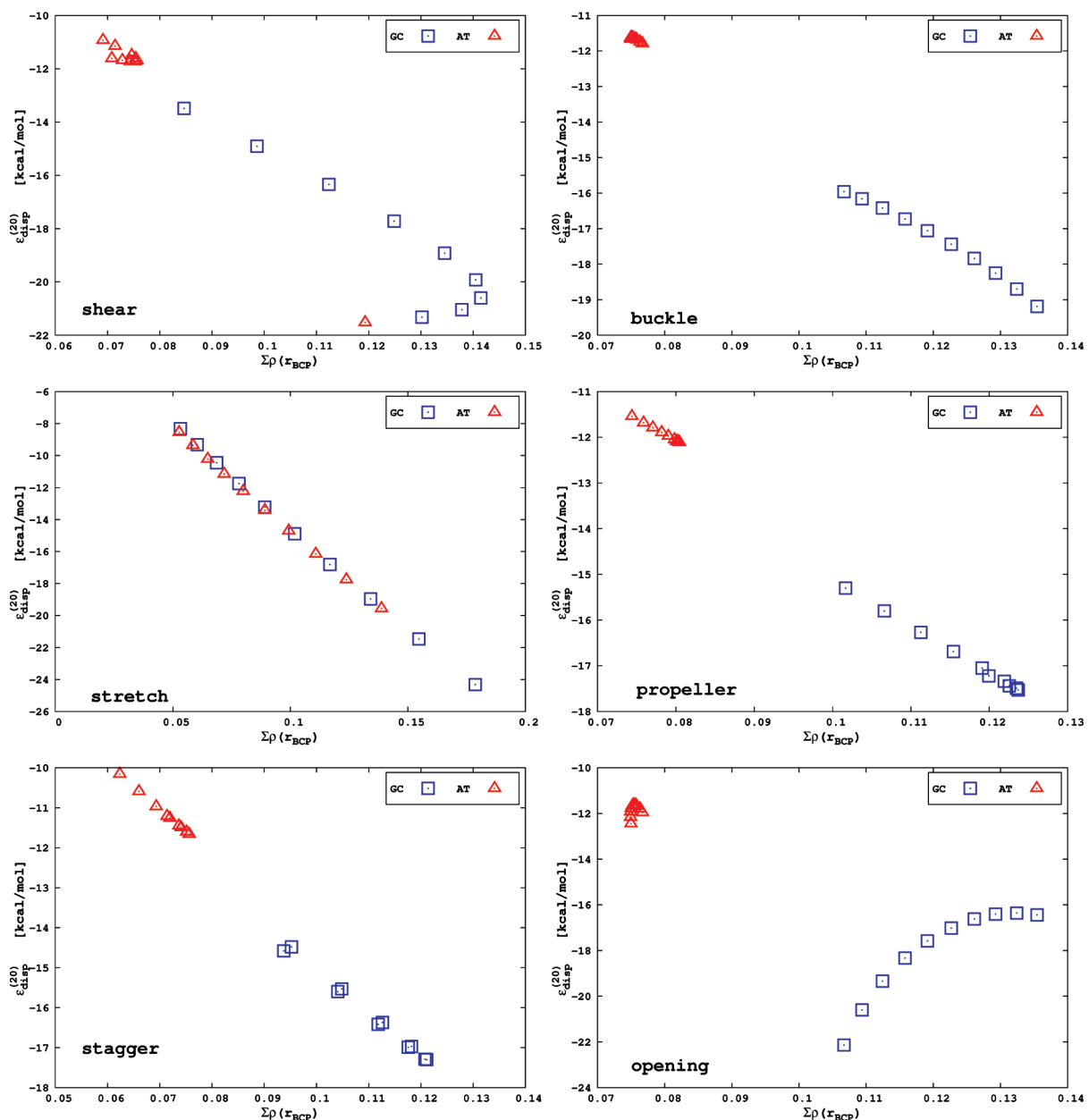


Figure 10. Dependence of dispersion energy on the sum of electron densities at hydrogen-bond critical points.

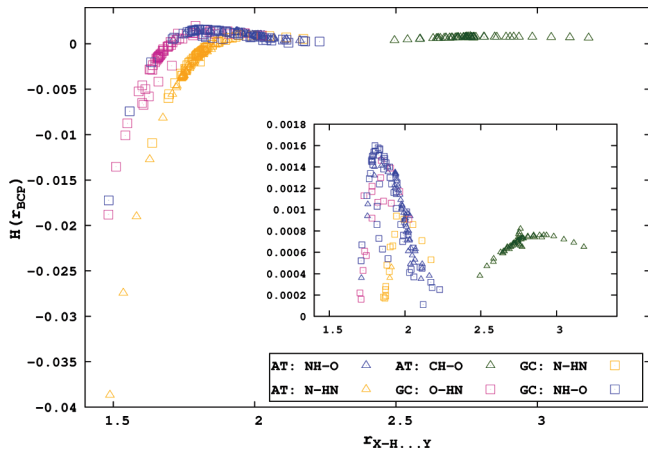


Figure 11. Dependence of $H(r)$ at $X-H \cdots Y$ bond critical point on the bond distance.

same is true for A-T NH \cdots O, G-C O \cdots HN, and G-C NH \cdots O hydrogen bonds. Among the two bonds, namely NH \cdots N and

NH \cdots O, the larger value of the electron density at the hydrogen bond critical point in the former case (for the same XH \cdots Y distance) is indicative of greater HB strength. The difference between the aforementioned bonds grows as the XH \cdots Y distance decreases. In Figure 9 one can see that the $\rho(\mathbf{r})$ values for the CH \cdots O interaction in the A-T base pair are clustering at definitely lower ranges of the electron density ($\rho(\mathbf{r}) < 0.09$ au) and greater distances of the XH \cdots Y bond than in the NH \cdots O and NH \cdots N bonds. Although the relations between various topological parameters of the electronic density and the intermolecular perturbation theory are by no means straightforward, an interesting observation can be made if we recall the consequences of multipole expansion of IIE components. Generally, the IIE and its components can be decomposed into a power series of the inverse of intermolecular distance R . Since the densities at BCPs correlate strongly with the strength of interaction, one would expect a similar dependence on R . As it turns out, a very good quality of nonlinear least-squares fit is obtained already for the functions having the general form of

TABLE 7: Topological Properties (in au) of the CHO Contact Critical Points in the A-T Base Pair

shear (Å)	$\rho(\mathbf{r})$	$\nabla^2\rho(\mathbf{r})$	stretch (Å)	$\rho(\mathbf{r})$	$\nabla^2\rho(\mathbf{r})$	stagger (Å)	$\rho(\mathbf{r})$	$\nabla^2\rho(\mathbf{r})$
buckle (deg)	$\rho(\mathbf{r})$	$\nabla^2\rho(\mathbf{r})$	propeller (deg)	$\rho(\mathbf{r})$	$\nabla^2\rho(\mathbf{r})$	opening (deg)	$\rho(\mathbf{r})$	$\nabla^2\rho(\mathbf{r})$
-0.337	0.00552	0.02074	-0.36	0.00990	0.03110	-0.57	0.00362	0.01398
-0.258	0.00563	0.02077	-0.32	0.00899	0.02875	-0.46	0.00398	0.01515
-0.178	0.00572	0.02075	-0.27	0.00818	0.02669	-0.35	0.00437	0.01634
-0.099	0.00578	0.02064	-0.22	0.00743	0.02473	-0.25	0.00473	0.01742
-0.020	0.00582	0.02052	-0.17	0.00676	0.02296	-0.14	0.00512	0.01851
0.060	0.00583	0.02033	-0.13	0.00614	0.02130	-0.04	0.00547	0.01950
0.139	0.00581	0.02008	-0.08	0.00556	0.01970	0.07	0.00582	0.02042
0.218	0.00577	0.01979	-0.03	0.00505	0.01825	0.17	0.00614	0.02124
0.298	0.00571	0.01949	0.01	0.00460	0.01690	0.28	0.00642	0.02196
0.377	0.00563	0.01913	0.06	0.00416	0.01557	0.39	0.00666	0.02257
<hr/>								
-7.24	0.00648	0.02196	-17.76	0.00554	0.01968	-7.02	0.00237	0.00978
-5.41	0.00635	0.02166	-15.38	0.00589	0.02059	-5.52	0.00271	0.01100
-3.57	0.00623	0.02136	-13.00	0.00620	0.02137	-4.02	0.00311	0.01236
-1.74	0.00612	0.02111	-10.63	0.00648	0.02208	-2.52	0.00357	0.01387
0.09	0.00601	0.02087	-8.25	0.00673	0.02267	-1.03	0.00409	0.01551
1.93	0.00591	0.02063	-5.87	0.00690	0.02309	0.47	0.00470	0.01733
3.76	0.00580	0.02038	-3.50	0.00702	0.02336	1.97	0.00540	0.01928
5.59	0.00572	0.02020	-1.12	0.00708	0.02349	3.47	0.00618	0.02137
7.43	0.00563	0.02000	1.26	0.00707	0.02348	4.97	0.00708	0.02367
9.26	0.00554	0.01980	3.64	0.00701	0.02332	6.47	0.00812	0.02622

$\rho(R) = A/R^n$. Interestingly, very similar parameters ($A \approx 0.4$ and $n \approx 4$) are obtained for almost all the above types of hydrogen bonds except of CH \cdots O ($A \approx 1.7$ and $n \approx 6$), which would suggest a slightly different nature of interactions for this type of bonds. These findings are also consistent with the nature of interactions discussed in the previous section, since one would expect values of the power n between 3 (due to the leading dipole–dipole component of the electrostatic interactions) and 6 (for induction and dispersion interactions).

In order to gain an insight into the nature of interactions between A-T and G-C base pairs and, in particular, to relate it to hydrogen bonding, we studied thoroughly the dependence of the total intermolecular interaction energy and its components on the sum of electron densities in the XH \cdots Y BCPs. Our recent study devoted to nucleic acid base-amino acid side-chain complexes showed the linear dependence of the total interaction energy on the sum of $\rho(\mathbf{r})$ in the BCPs.⁸⁷ In the case of the complexes analyzed here, no such correlations could be found with the exception of propeller parameter for which the correlation coefficients amount to 0.997 and 0.985 for A-T and G-C base pairs, respectively. This is most likely due to the fact that in our previous study we have investigated complexes at their equilibrium geometries (or close to it). Furthermore, the analyzed topological parameters and particularly the electron density at BCPs depend strongly on the geometrical parameters of hydrogen bonds, which for some of the scanned structural parameters of NAB complexes undergo nonlinear and sometimes opposite changes. Notably, there are many structures with hydrogen bonds far from linear arrangements. Among the considered components of the intermolecular interaction energy, only the dispersion term might be considered to depend linearly on the electron density. More precisely, the dependence is observed in case of buckle, propeller, stagger, and stretch parameters (see Figure 10). It is worth noting that the linear fit for the variation of the dispersion term with the sum of $\rho(\mathbf{r})$ at XH \cdots Y BCPs is exactly the same for A-T and G-C in the case of the stretch parameter.

The nature of the bonded interactions can be also characterized by the values of the Laplacian of the electron density $\nabla^2\rho(\mathbf{r})$ and the total energy density $H(\mathbf{r})$, which is a sum of the electron kinetic $G(\mathbf{r})$ and potential $V(\mathbf{r})$ energy densities. The shared

interactions may be quantitatively characterized by the two following criteria, namely $\nabla^2\rho(\mathbf{r}) < 0$, and $H(\mathbf{r}) < 0$. On the other hand the closed-shell interactions fulfill the following conditions: $\nabla^2\rho(\mathbf{r}) > 0$, and $H(\mathbf{r}) > 0$. The intermediate region (partially covalent interactions) is characterized by $\nabla^2\rho(\mathbf{r}) > 0$, and $H(\mathbf{r}) < 0$.^{88,89} In all considered cases $\nabla^2\rho(\mathbf{r})$ is positive but $H(\mathbf{r})$ assumes both positive and negative values. Figure 11 shows the relationship between $H(\mathbf{r})$ and XH \cdots Y distance. As mentioned previously, of the two bonds NH \cdots N and NH \cdots O, the former appears to be much stronger. The change of the interaction type between closed-shell and partially covalent bonds occurs at greater lengths of NH \cdots N hydrogen bonds than it does for NH \cdots O interaction (1.858 and 1.707 Å, respectively). Indeed, as it was shown by Matta et al., although the NH \cdots N bonds in both types of WC complexes exhibit hallmarks of closed-shell bonding at these distances, a certain degree of electron sharing is also observed.⁹⁰ It is also worth mentioning that in the case of shear parameter, the $H(\mathbf{r})$ values for the NH \cdots O bonds in G-C base pairs do not follow the same trends as in the case of the G-C O \cdots HN and A-T NH \cdots O bonds. The same is true for the CH \cdots O bonds.

The theoretical method of compliance constants implies that the CH \cdots O contact may be considered as a hydrogen bond with a weak interaction strength in the A-T base pair.^{91,92} However, the existence of the CH \cdots O hydrogen bond in the A-T base pair has been recently questioned.^{93,94} Therefore, it might be worth noting that, only in the case of 5 out of 60 A-T base pairs analyzed here, the values of the $\rho(r)$ and $\nabla^2\rho(\mathbf{r})$ fulfill the Koch and Popelier criteria for the existence of H-bonds (i.e., 0.002–0.034 au for electron density at BCP and 0.024–0.139 au for its corresponding Laplacian).⁸⁰ They are satisfied only for the highest value of the opening parameter and for the four lowest values of the stretch parameter (see Table 7). The data presented in Table 7 support the hypothesis that CH \cdots O contact in the A-T base pair can be considered as van der Waals interaction rather than a hydrogen-bonding interaction.⁹⁵

Summary

In this paper we discuss the nature of intermolecular interactions in Watson–Crick guanine–cytosine and adenine–thymine

base pairs for conformations appearing in B-DNA crystals. We performed an extensive analysis of the effect of conformational variability on IIE components and various QTAIM descriptors based on a set comprising more than 200 Watson–Crick base pairs.

The most evident general conclusion is that, even though the first-order electrostatic energy, $\epsilon_{\text{el}}^{(10)}$, is usually the largest stabilizing component, it is completely canceled out by the associated exchange repulsion in majority of the studied structures. As a result, the analyzed complexes of the nucleic acid bases appeared to be stabilized mainly by the delocalization component of the intermolecular interaction energy.

Perhaps a clarification is needed on why we insist upon such an interpretation of the results. One must keep in mind that the $\epsilon_{\text{el}}^{(10)}$ represents the electrostatic attraction of the unperturbed monomer charge densities, estimated in the so-called polarization approximation. Approximation neglecting the electron exchange effects among interacting species is appropriate for large intermolecular separations but is simply invalid once the monomer wave functions begin to overlap. Only proper antisymmetrization of the Hartree product of monomer wave functions allows to quantify the exchange effects and estimate the ΔE^{HL} interaction energy, which is repulsive for the vast majority of the considered structures. It should be emphasized that $\Delta E_{\text{del}}^{\text{HF}}$ quantifies the effects of mutual polarization of monomer charge densities and the associated Pauli repulsion. Therefore, it is more appropriate to compare this term with the ΔE^{HL} rather than with the $\epsilon_{\text{el}}^{(10)}$. The analyzed Watson–Crick structures are further stabilized by the dispersion energy, which remains an important stabilizing factor in the whole range of investigated structural parameters, even though it is significantly damped by the exchange-correlation effects. However, our results indicate that in some of the regions of configurational space the electron correlation effects are much more important and become the main origin of stabilization.

The anisotropy of interactions for A-T complexes is significantly smaller in comparison with G-C base pairs and only in the case of the stretch parameter one finds a similar relative changes of the interaction energy terms for both complexes. Generally, the IIE and its components depend more strongly on the translational parameters, particularly stretch and shear.

The analyzed topological parameters of the electron density and particularly hydrogen bond critical points in the studied Watson–Crick complexes indicate a partially covalent character of NH \cdots N and NH \cdots O H-bonds for smaller intermolecular separations. The change of the interaction type between closed-shell and partially covalent bonds occurs at slightly greater lengths of NH \cdots N hydrogen bonds than it does for NH \cdots O. Consistently, the former of the two bonds appears to be much stronger. A totally different nature of interactions is observed for the A-T CH \cdots O bonds. In fact, only in the case of 5 out of 60 A-T base pairs analyzed here do the values of the $\rho(r)$ and $\nabla^2\rho(r)$ fulfill the Koch and Popelier criteria for the existence of H-bonds.

As a part of a model study, we have also performed extensive testing of the UBDB+EPMM method. It was shown that this approach reliably predicts the electrostatic energy for Watson–Crick base pairs at a considerable saving in computation time.

Acknowledgment. This work was supported by computational grants from Wroclaw Center for Networking and Supercomputing (WCSS) and ACK Cyfronet. Work in Poland was financed by Wroclaw University of Technology while work in the USA was supported by grant no. HRD-0833178. R.Z. is

the recipient of the fellowship cofinanced by European Union within European Social Fund. P.M.D. and K.N.J. acknowledge support from a grant from Iceland, Liechtenstein, and Norway through the EEA Financial Mechanism and the HOMING Programme from the Foundation for Polish Science (Edition 2007).

Supporting Information Available: Structural base-pair parameters for the selected set of crystallographic complexes. This material is available free of charge via the Internet at <http://pubs.acs.org>.

References and Notes

- Dabkowska, I.; Gonzales, H. V.; Jurečka, P.; Hobza, P. *J. Phys. Chem. A* **2005**, *109*, 1131–1136.
- Kubař, T.; Hanus, M.; Ryjáček, F.; Hobza, P. *Chem.—Eur. J.* **2006**, *12*, 280–290.
- Mathews, D. H.; Sabina, J.; Zuker, M.; Turner, D. H. *J. Mol. Biol.* **1999**, *288*, 911–940.
- Seeman, N. C.; Rosenberg, J. M.; Rich, A. *Proc. Natl. Acad. Sci. U.S.A.* **1976**, *73*, 804–808.
- Šponer, J.; Riley, K. E.; Hobza, P. *Phys. Chem. Chem. Phys.* **2008**, *10*, 2595–2610.
- Hobza, P.; Šponer, J. *J. Am. Chem. Soc.* **2002**, *124*, 11802–11808.
- Jurečka, P.; Hobza, P. *J. Am. Chem. Soc.* **2003**, *125*, 15608–15613.
- Jurečka, P.; Šponer, J.; Hobza, P. *J. Phys. Chem. B* **2004**, *108*, 5466–5471.
- Jurečka, P.; Nachtigall, P.; Hobza, P. *Phys. Chem. Chem. Phys.* **2001**, *3*, 4578–4582.
- Jurečka, P.; Šponer, J.; Černý, J.; Hobza, P. *Phys. Chem. Chem. Phys.* **2006**, *8*, 1985–1993.
- Kabeláč, M.; Valdes, H.; Sherer, E. C.; Cramer, C. *J. Phys. Chem. Chem. Phys.* **2007**, *9*, 5000–5008.
- Sivanesan, D.; Sumathi, I.; Welsh, W. *J. Chem. Phys. Lett.* **2003**, *367*, 351–360.
- Xue, C.; Popelier, P. L. A. *J. Phys. Chem. B* **2009**, *113*, 3245–3250.
- Czyżnikowska, Ź.; Zaleśny, R.; Ziolkowski, M.; Gora, R. W.; Cysewski, P. *Chem. Phys. Lett.* **2007**, *450*, 132–137.
- Czyżnikowska, Ź.; Zaleśny, R.; Cysewski, P. *Pol. J. Chem.* **2008**, *82*, 2269–2279.
- Czyżnikowska, Ź. *J. Mol. Struct. (THEOCHEM)* **2009**, *895*, 161–167.
- Czyżnikowska, Ź.; Zaleśny, R. *Biophys. Chem.* **2009**, *139*, 137–143.
- Langner, K. M.; Sokalski, W. A.; Leszczynski, J. *J. Chem. Phys.* **2007**, *127*, 111102.
- Cysewski, P.; Czyżnikowska, Ź.; Zaleśny, R.; Czeleń, P. *Phys. Chem. Chem. Phys.* **2008**, *10*, 2665–2672.
- Hill, G.; Forde, G.; Hill, N., Jr.; Sokalski, W. A.; Leszczynski, J. *Chem. Phys. Lett.* **2003**, *381*, 729–732.
- Sedlák, R.; Jurečka, P.; Hobza, P. *J. Chem. Phys.* **2007**, *127*, 075104.
- Cybulska, H.; Sadlej, J. *J. Chem. Theory Comput.* **2008**, *4*, 892–897.
- Hesselmann, A.; Jansen, G.; Schütz, M. *J. Am. Chem. Soc.* **2006**, *128*, 11730–11731.
- Ran, J.; Hobza, P. *J. Phys. Chem. B* **2009**, *113*, 2933–2936.
- Tocylowski, R. R.; Cybulski, S. *J. Phys. Chem. A* **2003**, *107*, 418–426.
- Tocylowski, R. R.; Cybulski, S. *J. Chem. Phys.* **2005**, *123*, 154312.
- Mo, Y. *J. Mol. Model.* **2006**, *12*, 665–672.
- Chałasiński, G.; Szczęśniak, M. M. *Mol. Phys.* **1988**, *63*, 205.
- Cybulski, S. M.; Chałasiński, G.; Moszyński, R. *J. Chem. Phys.* **1990**, *92*, 4357.
- Dabkowska, I.; Jurečka, P.; Hobza, P. *J. Chem. Phys.* **2005**, *122*, 204322.
- Šponer, J.; Jurečka, P.; Hobza, P. *J. Am. Chem. Soc.* **2004**, *126*, 10142–10151.
- Rejnek, J.; Hobza, P. *J. Phys. Chem. B* **2007**, *111*, 641–645.
- Šponer, J.; Hobza, P. *J. Phys. Chem. A* **2000**, *104*, 4592–4597.
- Pitoňák, M.; Riley, K. E.; Neogrády, P.; Hobza, P. *ChemPhysChem* **2008**, *9*, 1636–1644.
- Pitoňák, M.; Neogrády, P.; Černý, J.; Grimme, S.; Hobza, P. *ChemPhysChem* **2009**, *10*, 282–289.
- Gilli, G.; Bellucci, F.; Ferretti, V.; Bertolasi, V. *J. Am. Chem. Soc.* **1989**, *111*, 1023.
- Gilli, G.; Bertolasi, V.; Ferretti, V.; Gilli, G. *J. Am. Chem. Soc.* **2000**, *122*, 10405–10417.

- (38) Gilli, G.; Bertolasi, V.; Pretto, L.; Lycka, A.; Gilli, G. *J. Am. Chem. Soc.* **2002**, *125*, 13554–13567.
- (39) Mohajeri, A.; Nobandegani, F. F. *J. Phys. Chem. A* **2008**, *112*, 281–295.
- (40) Bader, R. F. W. *Atoms In Molecules, A Quantum Theory*; Oxford University Press: Oxford, UK, 1990.
- (41) Popelier, P. *Atoms in Molecules, An Introduction*; Pearson Education Ltd: Upper Saddle River, NJ, 2000.
- (42) Matta, C. F., Boyd, R. J., Eds.; *The Quantum Theory of Atoms in Molecules: From Solid State to DNA and Drug Design*; Wiley VCH: Weinheim, Germany, 2007.
- (43) Grimme, S.; Antony, J.; Schwabe, T.; Mück-Lichtenfeld, C. *Org. Biomol. Chem.* **2007**, *5*, 741–758.
- (44) Antony, J.; Grimme, S. *Phys. Chem. Chem. Phys.* **2006**, *8*, 5287–5293.
- (45) Grimme, S.; Mück-Lichtenfeld, C.; Antony, J. *Phys. Chem. Chem. Phys.* **2008**, *10*, 3327–3334.
- (46) Korona, T.; Jeziorski, B. *J. Chem. Phys.* **2008**, *128*, 144107.
- (47) Korona, T. *Phys. Chem. Chem. Phys.* **2007**, *9*, 6004–6011.
- (48) Korona, T.; Jeziorski, B. *J. Chem. Phys.* **2006**, *125*, 184109.
- (49) Koritsanszky, T.; Volkov, A.; Coppens, P. *Acta Crystallogr.* **2002**, *A58*, 464–472.
- (50) Volkov, A. V.; Li, X.; Koritsanszky, T.; Coppens, P. *J. Phys. Chem. A* **2004**, *108*, 4283–4300.
- (51) Dominiak, P. M.; Volkov, A. V.; Li, X.; Messeschmidt, M.; Coppens, P. *J. Chem. Theory Comput.* **2007**, *3*, 232–247.
- (52) Volkov, A.; Koritsanszky, T.; Coppens, P. *Chem. Phys. Lett.* **2004**, *391*, 170–175.
- (53) Schmidt, M. W.; Baldridge, K. K.; Boatz, J. A.; Elbert, S. T.; Gordon, M. S.; Jensen, J. H.; Koseki, S.; Matsunaga, N.; Nguyen, K. A.; Su, S.; Windus, T. L.; Dupuis, M.; Montgomery, J. A. *J. Comput. Chem.* **1993**, *14*, 1347–1363.
- (54) Lu, X. J.; Olson, W. K. *Nucleic Acids Res.* **2003**, *31*, 5108–5121.
- (55) Berman, H. M.; Olson, W. K.; Beveridge, D. L.; Westbrook, J.; Gelbin, A.; Demeny, T.; Hsieh, S. H.; Srinivasan, A. R.; Schneider, B. *Biophys. J.* **1992**, *63*, 751–759.
- (56) Designed by: Friedrich, B.-K. *AIM2000 package*; University of Applied Sciences: Bielefeld, Germany.
- (57) Gutowski, M.; Duijneveldt, F. B.; Chałasiński, G.; Piela, L. *Mol. Phys.* **1987**, *61*, 223.
- (58) Sokalski, W. A.; Roszak, S.; Pecul, K. *Chem. Phys. Lett.* **1988**, *153*, 153.
- (59) Chałasiński, G.; Szcześniak, M. M. *Chem. Rev.* **1994**, *94*, 1723.
- (60) Gutowski, M.; Piela, L. *Mol. Phys.* **1988**, *64*, 337.
- (61) Frey, R. F.; Davidson, E. R. *J. Chem. Phys.* **1989**, *90*, 5555.
- (62) Moszyński, R. Theory of Intermolecular Forces: An Introductory Account. In *Molecular Materials with Specific Interactions—Modeling and Design*; Sokalski, W. A., Ed.; Springer: New York, 2007.
- (63) Moszyński, R.; Rybak, S.; Cybulski, S.; Chahasiński, G. *Chem. Phys. Lett.* **1990**, *166*, 609.
- (64) Hirschfelder, J. *Chem. Phys. Lett.* **1967**, *1*, 325.
- (65) Boys, S. F.; Bernardi, F. *Mol. Phys.* **1970**, *19*, 553.
- (66) Gora, R. W.; Bartkowiak, W.; Roszak, S.; Leszczynski, J. *J. Chem. Phys.* **2002**, *117*, 1031.
- (67) Gora, R. W.; Bartkowiak, W.; Roszak, S.; Leszczynski, J. *J. Chem. Phys.* **2004**, *120*, 2802.
- (68) Gora, R. W.; Sokalski, W. A.; Leszczynski, J.; Pett, V. B. *J. Phys. Chem. B* **2005**, *109*, 2027.
- (69) Gora, R. W. DENDIF package, Revision 2.1.2, Wrocław, Poland, 2001,
- (70) Schaftenaar, G.; Noordik, J. H. *J. Comput.-Aided Mol. Des.* **2000**, *14*, 123.
- (71) Volkov, A.; Messerschmidt, M. *Acta Crystallogr.* **2007**, *D63*, 160–170.
- (72) Li, X.; Volkov, A. V.; Szalewicz, K.; Coppens, P. *Acta Crystallogr.* **2006**, *D62*, 639–647.
- (73) Dominiak, P. M.; Volkov, A. V.; Dominiak, A. P.; Jarzembska, K. N.; Coppens, P. *Acta Crystallogr.* **2009**, *D65*, 485–499.
- (74) Volkov, A. V.; King, H. F.; Coppens, P. *J. Chem. Theory Comput.* **2006**, *2*, 81–89.
- (75) Faerman, C. H.; Price, S. L. *J. Am. Chem. Soc.* **1990**, *112*, 4915–4926.
- (76) Volkov, A.; Macchi, P.; Farrugia, L. J.; Gatti, C.; Mallinson, P.; Richter, T.; Koritsanszky, T. XD2006—A Computer Program Package for Multipole Refinement, Topological Analysis of Charge Densities and Evaluation of Intermolecular Energies from Experimental and Theoretical Structure Factors, 2006.
- (77) Gora, R. W.; Grabowski, S. J.; Leszczynski, J. *J. Phys. Chem. A* **2005**, *109*, 6397–6405.
- (78) Beck, J. F.; Mo, Y. *J. Comput. Chem.* **2007**, *28*, 455–466.
- (79) Bader, R. F. W. *Chem. Rev.* **1991**, *91*, 893.
- (80) Koch, U.; Popelier, P. L. A. *J. Phys. Chem.* **1995**, *99*, 9747–9754.
- (81) S. J. Grabowski, W. A.; Sokalski, J. L. *J. Phys. Chem. A* **2005**, *109*, 4331–4341.
- (82) Grabowski, S. J. *J. Phys. Chem. A* **2000**, *104*, 5551–5557.
- (83) Grabowski, S. J.; Sokalski, W. A.; Dyguda, E.; Leszczynski, J. *J. Phys. Chem. B* **2006**, *110*, 6444–6446.
- (84) Gu, J.; Wang, J.; Leszczynski, J. *J. Am. Chem. Soc.* **2004**, *126*, 12651–12660.
- (85) Parthasarathi, R.; Amutha, R.; Subramanian, V.; Nair, B. U.; Ramasami, T. *J. Phys. Chem. A* **2004**, *108*, 3817–3828.
- (86) Espinosa, E.; Molins, E.; Lecomte, C. *Chem. Phys. Lett.* **1998**, *285*, 170–173.
- (87) Czyżnikowska, Ź; Lipkowski, P.; Gora, R. W.; Zaleśny, R.; Cheng, A. C. *J. Phys. Chem. B* **2009**, *113*, 11511–11520.
- (88) Cremer, D.; Kraka, E. *Angew. Chem., Int. Ed.* **1984**, *23*, 637.
- (89) Arnold, W. D.; Oldfield, E. *J. Am. Chem. Soc.* **2000**, *122*, 12835.
- (90) Matta, C. F.; Castillo, N.; Boyd, R. J. *J. Phys. Chem. B* **2006**, *110*, 563–578.
- (91) Grunenberg, J. *J. Am. Chem. Soc.* **2004**, *126*, 16310–16311.
- (92) Brandhorst, K.; Grunenberg, J. *ChemPhysChem* **2007**, *8*, 1151–1156.
- (93) Shishkin, O. V.; Sponer, J.; Hobza, P. *J. Mol. Struct. (THEOCHEM)* **1999**, *477*, 15–21.
- (94) Guerra, C. F.; Bickelhaupt, F. M.; Snijders, J. G.; Baerends, E. J. *Chem.—Eur. J.* **1999**, *5*, 3581.
- (95) Zhou, P.-P.; Qiu, W.-Y. *J. Phys. Chem. A* **2009**, *113*, 10306–10320.

JP101258Q